Theoret. Chim. Acta (Berl.) 62, 245–255 (1983)

THEORETICA CHIMICA ACTA

Intrinsic Reaction Coordinate for the Gas-Phase Pyrolysis of Ethyl Formate

Kazuhiro Ishida and Shoichi Mayama

Department of Chemistry, Faculty of Science, Science University of Tokyo, Tokyo 162, Japan

Fukui's IRC is obtained for the pyrolysis of ethyl formate within the level of MNDO molecular orbital calculations. The activation enthalpy and entropy can be evaluated from the calculated partition functions and compared with the observed values. It is suggested that the pyrolysis would be significantly promoted when it occurs in an aprotic polar solvent.

Key words: Intrinsic reaction coorinate – Ethyl formate – Gas phase pyrolysis – Activation entropy – MNDO molecular orbital calculations.

1. Introduction

Generally a gas-phase reaction can be described by a potential-energy surface. However, obtaining a whole potential-energy surface requires great labor. The degree of freedom (or dimension) of the energy surface is 3N-6 for an N atomic system. If only ten grid-points for each variable (coordinate) are enough in order to describe the surface, we would need to compute up to 10^{3N-6} points (10^{27} points for an eleven atomic system). Thus it is impractical to compute a whole surface for a general reaction system. Chemical intuition usually reduces the difficulty.

In 1970, Fukui [1] suggested one method to solve the above problem. He proposed the theory of intrinsic reaction coordinate (IRC) which describes the reaction path on the energy surface. He and his co-workers have developed this theory and applied it to many reaction systems [2]. The IRC is the minimum energy path connecting reactants and products via the transition state (TS) on the mass-weighted potential-energy surface. McIver and Komornicki [3] suggested a definition of the TS on the energy surface. A practical method to trace

0040-5744/83/0062/0245/$02.20

the IRC has been proposed in a previous paper [4]. The TS can be obtained by McIver–Komornicki method [3].

Though TS gives us much information about the reactions, IRC should be computed simultaneously. The reason for this may be shown as follows: For the case in which we reach an intermediate of a reaction in tracing IRC starting from a given TS, we would require another TS. When we reach the other reactants (or products) in tracing IRC, the given TS is not the true TS for this reaction. Once we reach the specific reactants or products under consideration, the given TS can be confirmed.

In the present paper, IRC (containing TS as a stationary point) is obtained for a gas-phase pyrolysis of ethyl formate molecule to formic acid and ethylene molecules as products.

It is confirmed that the calculated IRC in one direction reaches the reactant in its cis-conformation and in the other direction reaches the products which have enough distance between them. Experimentally it has been confirmed that the reaction mechanism for the gas-phase pyrolysis of esters can be described in terms of a semi-polar six-membered cyclic TS [5]. Chuchani and his co-workers [6] demonstrated from kinetic measurements that the presence of a cyclohexene and/or propene, as free-radical inhibitors, causes no significant effect to the unimolecular rate of the pyrolysis. Thus this pyrolysis has not a radical but an ionic feature, even though in a gas-phase. The cyclic TS must be a prototype of TS for the series of the gas-phase pyrolysis of vinyl ethers and of N-alkyl amides [7].

To avoid excess labor, we adopted the MNDO molecular orbital method [8] to compute energies and energy-gradients on potential energy surfaces. It is well known that the MNDO method gives fairly good results in computing energies and vibrational wave numbers for many ground-state molecules [9]. The MNDO method may give, in some unfortunate cases, invalid results for the computation of a potential-energy surface [10]. However, it can be assumed that the MNDO surface is not invalid for the present case because of the ionic feature of the pyrolysis.

2. Structure of Transition States

Two TS are considered in the present calculations; i.e. six-membered and four-membered cyclic TS. Thermodynamic quantities of these TS and the reactant can be evaluated by the method described in the textbook by Herzberg [11]. The harmonic oscillator approximation is used for estimating the vibrational partition function. The high temperature approximation (equation (V, 29) in the textbook by Herzberg) is used for the rotational partition function. The electronic partition function is assumed to be unity both in the reactant and TS. Any correction for the internal rotations is not taken into account. Using the transition state theory, activation entropy $\Delta S^{\ddagger}$ and enthalpy $\Delta H^{\ddagger}$ can be derived from experimental Arrhenius parameters [12]. Though the TS theory may be some-

Table 1. Activation enthalpy and entropy at 298.15 K of the gas-phase pyrolysis of ethyl formate for six-membered and four-membered cyclic transition states comparing with experimental value

	$\Delta H^{\ddagger}$/kJmol^{-1}	$\Delta S^{\ddagger}$/JK^{-1} mol^{-1}
Four-membered TS	401	−10.3
Six-membered TS	335	−18.6
Experiment[a]	182	−36.3

[a] Ref. 12.

what doubtful for some limited cases [13], it would be valid for usual cases, at least for the present case. Table 1 shows the derived values of $\Delta S^{\ddagger}$ and $\Delta H^{\ddagger}$ as experimental values compared with those calculated from the partition functions computed. These values indicate that the six-membered cyclic TS (6-TS) is more favorable than the four-membered one (4-TS), which is consistent with experimental results [5, 12]. The absolute value of $\Delta H^{\ddagger}$ calculated for the 6-TS is significantly larger than experimental values. The reason would be mainly due to the defect of the MNDO method, particularly when applied to a system containing an intra-molecular hydrogen bond O —H---C as in the present case (see later): In such cases, the heat of formation ΔH_f° is evaluated disproportionally high as confirmed by the author in simpler systems (unpublished). It is well known that this feature is manifested by the MINDO/3 molecular orbital method [14]. Though the MNDO method can be considered as an improvement over the MINDO/3 method [15], the above situation will be the same.

Table 2 shows the three contributions to the absolute entropy at 298.15 K (in JK^{-1} mol^{-1}) for three states; the 4-TS, the 6-TS, and the reactant. In the ground state of ethyl formate (the reactant), the value of the rotational contribution to the entropy ($S^{\circ}_{\text{rot}} = 106.10$ JK^{-1}mol^{-1}) is consistent with that obtained from experimental rotational constants measured by Riveros and Wilson [16]: $S^{\circ}_{\text{rot}} = 105.83$ JK^{-1} mol^{-1}. The individual comparison in values of rotational constants is as follows: $A = 0.6339$ cm^{-1} (calc.) with 0.5919628 cm^{-1} (obs.); $B = 0.08992$ cm^{-1} (calc.) with 0.09689135 cm^{-1} (obs.); $C = 0.08122$ cm^{-1} (calc.) with 0.08603084 cm^{-1} (obs.). These observed values are converted from MHz to cm^{-1} using the value of 2.997925×10^{10} cm/s as the light velocity.

Table 2. Calculated translational, vibrational, and rotational contributions to the absolute entropy at 298.15 K (JK^{-1} mol^{-1})

	Reactant	6-TS[a]	4-TS[b]
S°_{trans}	162.45	162.45	162.45
S°_{vib}	53.55	34.18	41.90
S°_{rot}	106.10	105.82	106.48
S°_{total}	321.09	302.45	310.83

[a] Six-membered TS.

[b] Four-membered TS.

The difference in the absolute entropies between the reactant and the 6-TS, $\Delta S^{\ddagger}$, is mainly caused from the difference in vibrational entropies, as shown in Table 2. The computed vibrational wave numbers used for calculating vibrational partition functions are as follows:

3347, 3319, 3276, 3271, 3243, 3186, 2085, 1550, 1498, 1484, 1449, 1441, 1441, 1423, 1288, 1262, 1193, 1168, 1045, 1006, 881, 751, 418, 236, 218, 153, and 62 cm^{-1}

for the reactant molecule, and

3428, 3394, 3255, 3253, 3209, 2754, 1847, 1596, 1510, 1459, 1433, 1372, 1317, 1217, 1204, 1174, 1021, 949, 933, 864, 761, 567, 516, 469, 218, 104, and $844i$ cm^{-1} for the 6-TS.

The relatively small value of the imaginary wave number 844 i cm^{-1} shows that the potential-energy surface near the 6-TS is not very steep. The three minimum vibrational wave numbers for the reactant are 62, 153, and 218 cm^{-1}, which correspond to internal rotations (as torsional vibrations). The value of 62 cm^{-1} for the internal rotation of the ethyl group is consistent with the value of approximately 70 cm^{-1} estimated from the micro-wave measurement [16]. The normal coordinates corresponding to the above wave numbers are not presented here due to their many components [21].

For molecules with a number of symmetric tops attached to an essentially rigid frame, assuming free rotation, each top contributes a factor

$$Q_f = (8\pi^3 I_m kT)^{1/2}/nh, \tag{1}$$

to the partition function in addition to the total internal partition function, as described in the textbook by Herzberg [11]. The I_m is the reduced moment of inertia, and $n = 3$ for CH_3 group. Thus the rotation of the terminal CH_3 group corresponding to 153 cm^{-1} would contribute to the entropy by the additional term

$$S_{fr} = R(1/2 + \ln Q_f). \tag{2}$$

Now let us assume the value of the force constant K of the internal rotation to be 0.15 mdyn·Å as estimated experimentally by Shimanouchi and his co-workers [17], and evaluate the value of the reduced moment of inertia to be

$$I_m = K/(2\pi cw)^2 \tag{3}$$

where c is the light velocity and w is the wave number of 153 cm^{-1}. Thus $I_m = 1.80 \times 10^{-39}\ \mathrm{g \cdot cm^2}$, which gives $S_{fr} = 20.1\ \mathrm{JK^{-1}\,mol^{-1}}$. The rotation of the CH_3 group is not free but hindered so that the contribution to the entropy is less than the value of 20.1 $\mathrm{JK^{-1}\,mol^{-1}}$. However, it may be concluded that the discrepancy in $\Delta S^{\ddagger}$ (as shown in Table 1) is mainly due to the contribution from the internal rotations. The exact corrections for the internal rotations are not carried out in the present calculations.

The geometry fully optimized for the 6-TS is shown in Fig. 1. Atoms O_1 C_2 O_3 C_5 C_8 H_9 are almost on the same plane. Calculated atomic charges are shown in

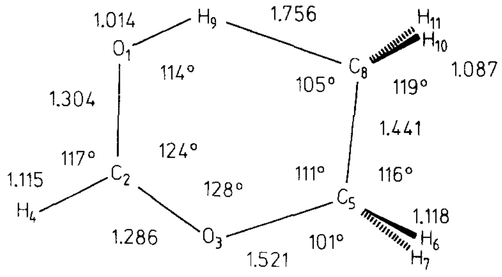

Fig. 1. Geometry of the six-membered cyclic transition state (A, deg.)

Table 3. In the 6-TS, the C_8—H_9 bond has already been broken heterolytically and an intra-molecular hydrogen-bond O_1 —H_9---C_8 has been formed. The O_3 —C_5 bond has been lengthened from 1.41 Å in the reactant to 1.52 Å in the 6-TS and will be broken heterolytically as shown in the next section. The highest occupied molecular orbital (HOMO) of the 6-TS is found to be a 2*p*-type MO localized at the C_8 atom tending toward the H_9 atom. Because the charge on the C_8 atom is −0.69 electron (see Table 3), the C_8 atom has a carbanion-like feature in the 6-TS. In order to confirm these heterolytic bond cleavages, Unrestricted Hartree–Fock calculations within the MNDO level were carried out for several geometries near the 6-TS and no differences from the Restricted Hartree–Fock (MNDO level) calculations were found.

The value of the dipole moment calculated for the 6-TS is 4.37 Debye. The polarity of the 6-TS is about 2.5 times greater than that of the reactant for which the value of 1.76 Debye can be calculated. The value of 1.76 Debye is consistent with the observed value of 1.98 ± 0.02 Debye [16]. The above fact might propose

Table 3. Calculated atomic charges for six-membered and four-membered cyclic transition states and for reactant

Atom[a]	6-TS[b]	4-TS[c]	Reactant
O_1	−0.26	−0.32	−0.36
C_2	0.46	0.33	0.38
O_3	−0.30	−0.29	−0.35
H_4	0.12	0.08	0.10
C_5	0.29	0.22	0.18
H_6	0.01	0.02	0.01
H_7	0.01	0.02	0.01
C_8	−0.69	−0.40	0.02
H_9	0.31	0.27	0.00
H_{10}	0.03	0.04	0.01
H_{11}	0.03	0.04	0.01

[a] For numbering, see Fig. 1 or Fig. 2.
[b] Six-membered cyclic transition state.
[c] Four-membered cyclic transition state.

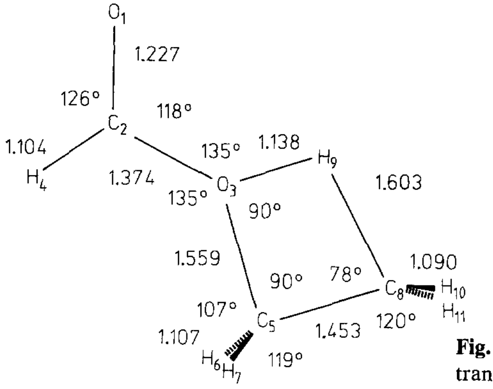

Fig. 2. Geometry of the four-membered cyclic transition state (A, deg.)

an experiment of kinetic measurements of the pyrolysis in an aprotic polar solvent. This point will be discussed in the next section.

Figure 2 shows the fully optimized geometry for the 4-TS. Atomic charges are shown in Table 3. The situation in the 4-TS is quite similar to that in the 6-TS. The intra-molecular hydrogen-bond O_3 $-H_9$---C_8 has been formed and the C_8 carbon atom resembles a carbanion. HOMO of the 4-TS is also a $2p$-type MO localized C_8 carbon atom tending toward the H_9 hydrogen atom. The O_3 $-C_5$ bond has been lengthened from 1.41 Å to 1.56 Å and will be broken heterolytically. The value of the dipole moment calculated for the 4-TS is 2.88 Debye. The calculated wave numbers for the 4-TS are as follows:

3419, 3390, 3327, 3302, 3285, 2276, 2062, 1540, 1466, 1446, 1380, 1309, 1267, 1189, 1116, 1075, 1035, 968, 942, 859, 643, 554, 501, 248, 166, 100, and $1904i$ cm^{-1}.

The imaginary wave number of $1904i$ cm^{-1} is relatively large and shows a steep precipice near the 4-TS on the energy surface. The calculated rotational constants for the 4-TS are as follows: $A = 0.6160$ cm^{-1}; $B = 0.08710$ cm^{-1}; $C = 0.07869$ cm^{-1}.

3. Analysis along Intrinsic Reaction Coordinate

The potential energy profile along IRC is shown in Fig. 3 for the pyrolysis via the 6-TS. Each point of IRC on the potential surface is indicated by the distance along IRC from TS; i.e., the TS is indicated by $s = 0.0$ and the minus (plus) sign of s denotes the reactant (product) region of reaction. The unit of IRC is (atomic mass unit)$^{1/2}$(Å). Along IRC, the energy is precipitously increased from that of the reactant up to that of the 6-TS and then gradually diminished to that of the products.

Table 4 shows atomic charges calculated along IRC. Key values among these charges are those of C_5, C_8, and H_9 atoms. The charge of the C_8 atom along IRC is steeply diminished from near neutral to −0.69 electron and then pre-

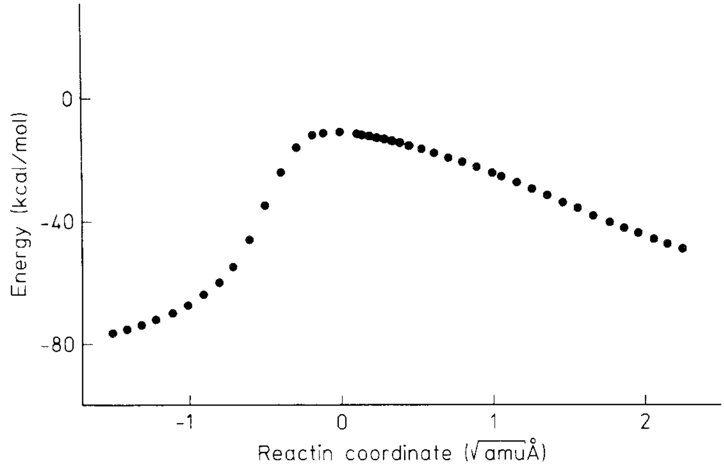

Fig. 3. Potential energy profile along IRC of the six-membered cyclic transition state

cipitously increased to −0.08 electron. The charge of the C_5 atom is gradually increased from 0.18 to 0.29 and then gradually diminished to −0.08. For the H_9 atom, the charge is steeply increased from neutral up to 0.31 and then gradually diminished to 0.22. The other charges are not significantly varied along IRC, as seen in Table 4. At IRC $s = +1.56$ (where the O_3 —C_5 bond distance is about 2 Å as shown in Table 5), the charge of the C_8 atom is −0.29 electron, which is mainly due to the localization of π electrons at the C_8 atom in the product ethylene molecule. Table 5 shows heat of formations, dipole moments, and several bond distances (O_1 —C_2, C_2 —O_3, O_3 —C_5, C_5 —C_8, C_8—H_9, and O_1 —H_9 bonds) calculated along IRC. The dipole moment along IRC is steeply increased from 1.76 Debye at the reactant up to 4.37 Debye at the 6-TS and then gradually diminished to 1.49 DebyeVat the products. The distance of the O_1—H_9 bond is gradually diminished along IRC to its final value of 0.950 Å. For the C_8—H_9 bond (also the O_3—C_5 bond), the distance is gradually increased along IRC to infinity. The distance of the O_1—C_2 bond is slightly increased from 1.225 Å (the double bond length of C=O) to 1.354 Å (the single bond length of C—O). To the contrary, the C_2—O_3 distance is slightly diminished from the single bond length to the double bond length. The distance of the C_5—C_8 bond is also diminished from the single bond length to the double bond length. In order to see the whole geometrical change along IRC, two figures are presented; Fig. 4 shows the geometry at IRC $s = -1.50$ and Fig. 5 shows the geometry at IRC $s = +1.56$. Thus, we can see the whole geometrical change along IRC by successively looking at Fig. 4, Fig. 1, and Fig. 5.

Thus, the feature of the pyrolysis is as follows: First the ethyl formate molecule rotates internally from its trans-conformation about the O_3—C_5 bond to its cis-conformation. Next the O_3 —C_5 bond is gradually stretched, breaking the C_8—H_9 bond heterolytically and forming the O_1 —H_9 bond. At the TS, a hydrogen bond of O_1 —H_9---C_8 is formed. Finally the O_3 —C_5 bond and the

Table 4. Calculated atomic charges along IRC of six-membered cyclic transition state[a]

Atom	Reactant	$s=-1.50$	$s=-1.01$	$s=-0.50$	$s=0.00$	$s=+0.62$	$s=+1.06$	$s=+1.56$	Products
O_1	−0.36	−0.37	−0.37	−0.37	−0.26	−0.28	−0.30	−0.31	−0.31
C_2	0.38	0.39	0.39	0.41	0.46	0.43	0.41	0.39	0.36
O_3	−0.35	−0.34	−0.35	−0.34	−0.30	−0.33	−0.36	−0.37	−0.37
H_4	0.10	0.10	0.09	0.10	0.12	0.11	0.10	0.09	0.11
C_5	0.18	0.18	0.19	0.23	0.29	0.23	0.17	0.11	−0.08
H_6	0.01	0.01	0.02	0.02	0.01	0.01	0.02	0.03	0.04
H_7	0.01	0.01	0.01	0.02	0.01	0.01	0.02	0.03	0.04
C_8	0.02	−0.03	−0.06	−0.28	−0.69	−0.53	−0.40	−0.29	−0.08
H_9	0.00	0.06	0.07	0.17	0.31	0.28	0.25	0.24	0.22
H_{10}	0.01	0.00	0.00	0.02	0.03	0.04	0.04	0.04	0.04
H_{11}	0.01	0.00	0.00	0.02	0.03	0.04	0.04	0.04	0.04

[a] For the notation of IRC, see text; for numbering of atoms, see Fig. 1.

Table 5. Calculated heat of formations, dipole moments, and several bond distances along IRC of the six-membered cyclic transition state[a]

	Reactant	$s=-1.50$	$s=-1.01$	$s=-0.50$	$s=0.00$	$s=+0.62$	$s=+1.06$	$s=+1.56$	Products
ΔH_f° kcal/mol	−91.0	−76.7	−67.5	−34.9	−11.0	−17.8	−25.6	−36.2	−77.4
Dipole moment (Debye)	1.76	1.41	1.44	1.86	4.37	3.13	2.11	1.39	1.49[b]
O_1—C_2 bond Å	1.225	1.225	1.227	1.265	1.304	1.328	1.337	1.344	1.354
C_2—O_3 bond Å	1.357	1.355	1.356	1.320	1.286	1.251	1.236	1.229	1.227
O_3—C_5 bond Å	1.409	1.406	1.425	1.447	1.521	1.681	1.814	1.975	∞
C_5—C_8 bond Å	1.540	1.542	1.529	1.486	1.441	1.383	1.361	1.348	1.335
C_8—H_9 bond Å	1.109	1.104	1.095	1.321	1.756	2.000	2.082	2.144	∞
O_1—H_9 bond Å	4.983	1.994	1.764	1.371	1.014	0.957	0.948	0.945	0.950

[a] See footnote of Table 4.

[b] Dipole moment of formic acid.

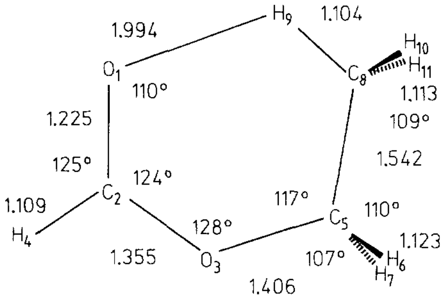

Fig. 4. Geometry at IRC $s = -1.50$ (A, deg.)

hydrogen bond are broken, resulting in a lone-pair orbital on the O_3 atom and a π orbital on C_5 and C_8 atoms.

The charge transfer of about 0.04 electron from ethylene to formic acid occurring at IRC $s = +1.56$ appears quite small so that the polarization effect in π electrons of ethylene is important while the charge transfer effect may not be important for the inverse reaction $HCOOH + C_2H_4 \rightarrow HCOOC_2H_5$. Thus in the addition reaction, the interaction of the lone-pair orbital of carbonyl oxygen in formic acid (HOMO) with π^* orbital of ethylene (the lowest unoccupied MO) would be essential and will cause the polarization of π electrons in ethylene, resulting in an electrostatic attractive force which acts as the driving force of the addition reaction. The Arrhenius activation energy of the addition reaction can be estimated to be 30.5 kcal·mol^{-1} in a gas-phase, because $\Delta H_f^\circ = -91.0$ kcal·mol^{-1} calculated for $HCOOC_2H_5$, $\Delta H_f^\circ = -77.4$ kcal·mol^{-1} calculated for $HCOOH + C_2H_4$, and the observed Arrhenius activation energy $E_a = 44.1$ kcal·mol^{-1} [12] for $HCOOC_2H_5 \rightarrow HCOOH + C_2H_4$. The syn-addition reaction of carboxylic acid to olefin would also be significantly promoted when it takes place in an aprotic polar solvent, as would the pyrolysis.

Now let us discuss the pyrolysis reaction in an aprotic polar solvent in more detail. Following Kirkwood [18], the rate constant k_s of the pyrolysis in an aprotic polar solvent with its dielectric constant D as a continuum medium is approximately given by

$$\ln k_s = \ln k_g - \frac{1}{RT}\frac{D-1}{2D+1}\left\{\frac{\mu^2}{r^3} - \frac{(\mu^\ddagger)^2}{(r^\ddagger)^3}\right\}, \tag{4}$$

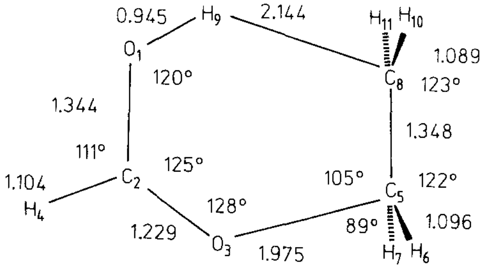

Fig. 5. Geometry at IRC $s = +1.56$ (A, deg.)

where k_g is rate constant in the gas-phase, μ ($\mu^{\ddagger}$) is the dipole moment of the reactant (of the 6-TS), and r ($r^{\ddagger}$) is the molecular radius of the reactant (of the 6-TS) as an imaginary sphere molecule. The gas-phase rate constant k_g is obtained from the kinetic measurements as

$$\ln k_g = \ln A - \frac{E_a}{RT}, \tag{5}$$

where $\ln A = 26.09$ and $E_a = 44.1\ \text{kcal mol}^{-1}$ [12]; i.e.,

$$\ln k_g = 26.09 - 22190/T. \tag{6}$$

For instance, $\ln k_g = -5.61$ at 700 K (the observed temperature region). The value of the dielectric constant D is always large for typical aprotic polar solvents; for instance, $D = 46.6$ for dimethyl sulfoxide, $D = 36.71$ for N,N-dimethyl formamide, and so on [19]. Thus the factor $(D-1)/(2D+1)$ in (4) is always nearly equal to $\frac{1}{2}$. Next, in order to evaluate r and $r^{\ddagger}$ in (4), let us assume the reactant molecule (also the 6-TS molecule) to be a sphere molecule of which the moment of inertia I (also $I^{\ddagger}$) is equal to the average of three principal moments of inertia of the reactant $I_A I_B I_C$ (also of the 6-TS: $I_A^{\ddagger} = 9.778 \times 10^{-39}\ \text{g}\cdot\text{cm}^2$; $I_B^{\ddagger} = 1.741 \times 10^{-38}\ \text{g}\cdot\text{cm}^2$; $I_C^{\ddagger} = 2.606 \times 10^{-38}\ \text{g}\cdot\text{cm}^2$); i.e. $I = 2.334 \times 10^{-38}\ \text{g}\cdot\text{cm}^2$ and $I^{\dagger} = 1.775 \times 10^{-38}\ \text{g}\cdot\text{cm}^2$. Generally a sphere of radius b with mass M has a moment of inertia of $(2/5)Mb^2$. Therefore, using $M = 74.0367$ atomic mass unit for the reactant and also for the 6-TS, we have $r = 2.179 \times 10^{-10}\ \text{m}$ and $r^{\ddagger} = 1.900 \times 10^{-10}\ \text{m}$. The above evaluation appears to be reasonable because these radii are about 2 Å. Thus, using the conversion factors; 1 Debye $= 3.33564 \times 10^{-30}\ \text{C}\cdot\text{m}$ and $1\ \text{C}^2\ \text{m}^{-1} = 5.412456 \times 10^{30}\ \text{kJ}\cdot\text{mol}^{-1}$, we have

$$\ln k_s = 26.09 - 13190/T. \tag{7}$$

For instance, $\ln k_s = -6.89$ at 400 K, which may be a measurable order of magnitude. The apparant Arrhenius activation energy derived from (7) would be 26.2 kcal mol^{-1} in any aprotic polar solvent. Although the above estimation of the rate constant k_s may be rough, it would be concluded that the pyrolysis reaction occurs in an aprotic polar solvent at a temperature of 400 K or less. Also the inverse reaction (syn-addition of carboxylic acid to olefin) could be observed at a temperature of 400 K or less in an aprotic polar solvent.

4. Summary

We can see in detail how ethyl formate reacts in the gas-phase pyrolysis. The calculated geometries, principal moments of inertia, vibrational wave numbers, and dipole moments would be fairly reasonable not only for the ground states but also for the transition states. It appears that the qualitative feature of the pyrolysis can be reasonably described from the present calculations since this feature is quite consistent with experimental results. Thus the MNDO molecular orbital method may be used in order to describe a qualitative feature of ionic reactions in gas-phase. It is found that the internal rotations contribute largely to entropy for the present reaction.

Although the present estimation may be rough, it appears that the pyrolysis is significantly promoted when it takes place in an aprotic polar solvent. The syn-addition of carboxylic acid to olefin may occur in an aprotic polar solvent.

Acknowledgement. The authors wish to thank Prof. Dr. Masao Kotani (the president of their university) for reading manuscript and for his valuable comments. The numerical calculations were carried out at the Computer Centre of the University of Tokyo and at the Computer Center of Institute for Molecular Science. All QCPE programs used were donated to the authors via IMS.

References

1. Fukui, K.: J. Phys. Chem. **74**, 4161 (1970).
2. For instance, see Fukui, K.: "The World of Quantum Chemistry", Reidel 1974 p. 113; Fukui, K., Kato, S., Fujimoto, H.: J. Am. Chem. Soc. **97**, 1 (1975); Kato, S., Fukui, K.: Am. Chem. Soc. **98**, 6395 (1976); Kato, S., Kato, H., Fukui, K.: Am. Chem. Soc. **99**, 684 (1977); Fukui, K., Koga, N., Fujimoto, H.: ibid. **103**, 196 (1981); Tachibana, A., Fukui, K.: Theoret Chim. Acta (Berl.) **49**, 321 (1978); ibid. **51**, 189 (1979); Theoret. Chim. Acta (Berl.) **51**, 275 (1979); ibid., **57**, 81 (1980); Yamashita, K., Kaminoyama, M., Yamabe, T., Fukui, K.: Theoret. Chim. Acta (Berl.) **60**, 303 (1981); Fujimoto, H., Fukui, K.: Israel J. Chem. **19**, 317 (1980); Fujimoto, H., Koga, N., Endo, M., Fukui, K.: Tetrahedron Letts. **22**, 1263 (1981)
3. McIver, J. W., Komornicki, A.: J. Am. Chem. Soc. **94**, 2625 (1972)
4. Ishida, K., Morokuma, K., Komornicki, A.: J. Chem. Phys. **66**, 2153 (1977)
5. Chuchani, G., Martin, I., Hernandez, J. A., Rotinov, A., Fraile, G., Bigley, D. B.: J. Phys. Chem. **84**, 944 (1980)
6. Martin, I., Chuchani, G., Avlla, I., Rotinov, A., Olmos, R.: J. Phys. Chem. **84**, 9 (1980)
7. For instance, see Maccoll, A., Nagra, S. S.: J. Chem. Soc. Faraday trans. I 1975, 2450
8. Dewar, M. J. S., Thiel, W.: J. Am. Chem. Soc. **99**, 4899 (1977); Q. C. P. E. No. 353
9. Dewar, M. J. S., Ford, G. P., McKee, M. L., Rzepa, H. S., Thiel, W., Yamaguchi, Y.: J. Mol. Struc. **43**, 135 (1978)
10. For instance, see Nagase, S., Ray, N. K., Morokuma, K.: J. Am. Chem. Soc. **102**, 4536 (1980)
11. Herzberg, G.: Molecular spectra and molecular structures. Vol. II. Infrared and raman spectra of polyatomic molecules. Chap. V, London: Van Nostrand Co. Inc., 1945
12. Maccoll A.: J. Chem. Soc. 1958, 3398
13. Golden, D. M.: J. Phys. Chem. **83**, 108 (1979)
14. For instance, see Zielinski, T. J., Breen, D. L., Rein, R.: J. Am. Chem. Soc. **100**, 6266 (1978); Klopman, G., Andreozzi, P., Hopfinger, A. J., Kikuchi, O., Dewar, M. J. S.: J. Am. Chem. Soc. **100**, 6267 (1978)
15. For instance, see Jug, K., Nanda, D. N.: Theoret. Chim. Acta (Berl.) **57**, 107 (1980); Theoret. Chim. Acta (Berl.) **57**, 131 (1980)
16. Riveros, J. M., Wilson, E. B.: J. Chem. Phys. **46**, 4605 (1967)
17. Shimanouchi, T., Matuura, H., Ogawa, Y., Harada, I.: J. Phys. Chem. Ref. Data **9**, 1149 (1980).
18. Kirkwood, J. G.: J. Chem. Phys. **2**, 351 (1934)
19. Janz, G. J., Tomkins, R. P. T.: Nonaqueous Electrolytes Handbook, Vol. I., Academic Press 1972
20. Nace, H. R.: J. Am. Chem. Soc. **81**, 5428 (1959)
21. They are available upon request to the authors

Received July 27, 1982